International Journal of Refractory Metals and Hard Materials 111 (2023) 106084

Contents lists available at ScienceDirect

International Journal of Refractory Metals and Hard Materials

journal homepage: www.elsevier.com/locate/IJRMHM

Fracture mechanics analysis of hardmetals by using artificial small-scale flaws machined at the surface through short-pulse laser ablation

L. Ortiz-Membrado [a], C. Liu [b,**], L. Cabezas [a], L.L. Lin [c], S. Fooladi Mahani [a], M.S. Wang [c], E. Jiménez-Piqué [a,d], L. Llanes [a,d,*]

[a] CIEFMA, Department of Materials Science and Engineering, Universitat Politècnica de Catalunya - BarcelonaTech, Campus Diagonal Besòs-EEBE, Barcelona 08019, Spain
[b] Xiamen Tungsten Co., Ltd., 361009 Xiamen, China
[c] Xiamen Golden Egret Special Alloy Co., Ltd., 361006 Xiamen, China
[d] Barcelona Research Center in Multiscale Science and Engineering, Universitat Politècnica de Catalunya - BarcelonaTech, Campus Diagonal Besòs, 08019 Barcelona, Spain

ARTICLE INFO

Keywords:
Fracture mechanics
Short pulse laser ablation
Micronotches
Small-scale flaws
Hardmetals

ABSTRACT

Laser ablation has become an innovative treatment for cemented carbides, regarding edge rounding and surface modification, aiming to improve their tribomechanical performance. Meanwhile, the precision offered for this technique has also positioned it as an effective mean to generate micronotches used for evaluation of mechanical properties in structural materials. However, similar approach has not been attempted for hardmetals; thus, it becomes the main objective of this work. Dimple-like and elongated micronotches are introduced in one fine-grained WC-11%wtCo grade. In doing so, laser processing parameters are first optimized to attain micronotches with appropriated geometry and size, i.e. similar to critical flaws identified in broken pristine specimens. Success of the implemented approach is then validated through subsequent flexural testing, fractographic inspection and fracture mechanics analysis of the results attained on samples containing surface micronotches, as far as laser-induced residual stresses are taken into consideration. In this regard, elongated micronotches are found to exhibit lower residual stresses, and postulate themselves as the optimal option of the two micronotch types studied. The suitability of laser ablation for shaping artificial small-scale flaws opens a new route for introducing controlled defects, alike those intrinsic to processing or induced during service, key aspect for further understanding damage tolerance issues in cemented carbides.

1. Introduction

In the last decades one of the main objectives of research concerned with structural ceramics, hardmetals and superhard materials, has relied on increasing reliability through creation of microstructures that impart sufficient fracture resistance so that strength becomes less sensitive to the size of flaws (e.g. Refs. [1–5]). This approach, different from the one simply based on flaw control, has the advantage that damage induced during service could be tolerated without compromising the reliability of the corresponding components.

Within the above framework, introduction of controlled damage has proven to be an effective route for studies addressing microstructural design optimization on the basis of damage tolerance. In doing so, spherical indentation have been successfully implemented in all above referred material groups, following protocols proposed and validated by Lawn's group (e.g. Refs. [6,7]). Meanwhile, surface machining by means of laser ablation has also emerged as an interesting option for introducing micrometric features in a controlled manner, such as small-scale notches, for evaluation of mechanical properties of metallic materials (e.g. Refs. [8–10]). For the particular case of cemented carbides, laser beam machining has shown to be capable of shaping small-scale features with precise dimensions and geometry with minimum microstructural changes and thermal damage. As a consequence, it has positioned as an effective route for post-processing and fabrication, surface texturing as

* Corresponding author at: CIEFMA, Department of Materials Science and Engineering, Universitat Politècnica de Catalunya - BarcelonaTech, Campus Diagonal Besòs-EEBE, Barcelona 08019, Spain.
** Corresponding author at: Xiamen Tungsten Co., Ltd., 361009 Xiamen, China.
E-mail addresses: liu.chao@cxtc.com (C. Liu), luis.miguel.llanes@upc.edu (L. Llanes).

https://doi.org/10.1016/j.ijrmhm.2022.106084
Received 5 October 2022; Received in revised form 9 December 2022; Accepted 9 December 2022
Available online 11 December 2022

well as micromachining of tools and components (e.g. Refs. [11–17]). Such application has recently been extended to machining of shallow and through-thickness micronotches of hardmetal specimens, within testing protocols for reliable assessment of fracture toughness in these hard and brittle-like materials [18].

Following the above ideas, it is the objective of this work to combine laser technology with the challenge of replicating damage induced during service-like conditions for analyzing the fracture mechanics of hardmetals containing controlled flaws. Although investigations on the interaction of laser pulses with solid materials have shown that heat diffusion into the surrounding material is reduced with decreasing pulse duration, it is also well-established that enhanced quality resulting by using shorter pulses is linked to higher ownership costs, more technical complexity and need of highly trained staff [e.g. Refs [19–21]. Hence, being aware of the compromise between accuracy limitation for shaping artificial processing-like flaws and practicability, accessibility and cost-effectiveness of the laser technology route chosen, the study is conducted by means of nanosecond laser ablation, i.e. within the short-pulse regime.

2. Experimental aspects

2.1. Material studied and mechanical properties

The study is conducted in a fine-grained (mean carbide size about 0.7 μm) WC-11%wtCo hardmetal grade. Hardness, fracture toughness and flexural strength for the investigated material are listed in Table 1. In general, measured values for these mechanical properties are within the range of those reported in the literature for WC-Co cemented carbides with similar microstructural assemblage (e.g. Refs. [22–25]). Mean and standard deviation values calculated for hardness are the result of ten indentations, measured using a Vickers diamond pyramidal indenter and an applied load of 30 kgf (294 N). Fracture toughness was evaluated following the single edge notched bend (SENB) method, using four rectangular bars of 45 × 10 × 5 mm dimensions and notch length-to-specimen width ratio of 0.3. The effective evaluation of fracture toughness using linear elastic fracture mechanics (LEFM) requires the suitability of a procedure for introducing a sharp pre-crack into the sample. In this work, it was achieved through application of cyclic compressive loads by reverse bending to a SENB specimen, followed by stable crack growth under far-field tensile stresses. The latter step was conducted to relieve residual stresses induced during the previous cyclic compression. A detailed description of the pre-cracking procedure used has been reported elsewhere [18,26,27]. Flexural strength was assessed by testing to failure fifteen rectangular bars with dimensions of 45 × 4 × 5 mm. It was conducted under four-point bending with inner and outer spans of 20 and 40 mm respectively. Before testing, the longitudinal section later subjected to the maximum stress in bending was ground and polished until mirror-like surface finish. Additionally, longitudinal edges of all the samples were beveled. All the mechanical tests (fatigue pre-cracking, fracture toughness and flexural strength) were conducted using a servohydraulic testing machine in a room air environment. Failure for all the unnotched specimens tested under flexure resulted in a very large number of broken fragments. Although an extensive examination was conducted in many of the broken pieces, in all the cases it was impossible to discern nature, geometry and size of the strength–limiting flaws. It points out that fracture originated from intrinsic microstructural heterogeneities. Within this context, critical flaw sizes were estimated to be about 10–20 μm, according to LEFM criterion, by assuming them to be embedded circular defects. This value is relevant for the study as it is taken as reference for defining length-scale of micronotches to be machined.

Table 1
Hardness, fracture toughness and flexural strength of the hardmetal grade studied.

Hardmetal grade	Hardness (GPa)	Fracture toughness (MPa $m^{1/2}$)	Flexural strength (MPa)
WC-11%$_{wt}$Co (d_{wc} = 0.7 μm)	15.4 ± 0.2	10.9 ± 0.3	3810 ± 361

2.2. Laser ablation machining of micronotches

A solid-state Nd:YLF, Q-switched laser set-up was employed to machine dimple-like and elongated micronotches on the target surfaces. The set-up is capable to emit laser beams having the wavelength of 349 nm and pulse duration of 5 ns. The laser machining platform consists of a 2-axis laser beam deflection unit that controls the movement of the focus point on the XY-plane, together with two mirrors that adjust the trajectory of the laser beams. The sample is fixed on the sample holder which is equipped with Vernier calipers along the x-, y- and z-axis.

Preliminary efforts concentrated on studying the influence of laser machining parameters – mainly number of passes (within a range between 1 and 10,000, in 10-times intervals) and frequency (values of 1 kHz, 3 kHz, 15 kHz and 150 kHz) - on geometry accuracy (Fig. 1). Optimized laser-ablation conditions were selected on the basis of combined and complementary optical and scanning electron microscopy inspection of all the machined micronotches, regarding well-defined aspect ratio geometry and dimensions of the aimed flaw-like features. Furthermore, as laser ablation may induce irreversible changes, special attention was paid to explore possible damage induced at the surface of the shaped micronotches. This surface integrity evaluation was conducted through Field Emission Scanning Electron Microscopy (FESEM).

Flexural strength was the parameter used to evaluate micronotching effects on the fracture resistance of the studied hardmetal. Mechanical testing was complemented by extensive fractography of all the broken samples. Fractographically derived micronotch information included detailed aspect ratio geometry and dimensions (length and depth) of micronotches acting as failure origins. The experimental data were then used for evaluating correspondence between observed and estimated flaw sizes, the latter calculated from the fundamental LEFM correlation among critical defect size, strength and fracture toughness. Inconsistent results were taken as an indicator of residual stress effects. Rough estimations of the residual stress level were assessed from the total stress intensity factor evaluated on the basis of the real failure-controlling crack system discerned by fractographic examination.

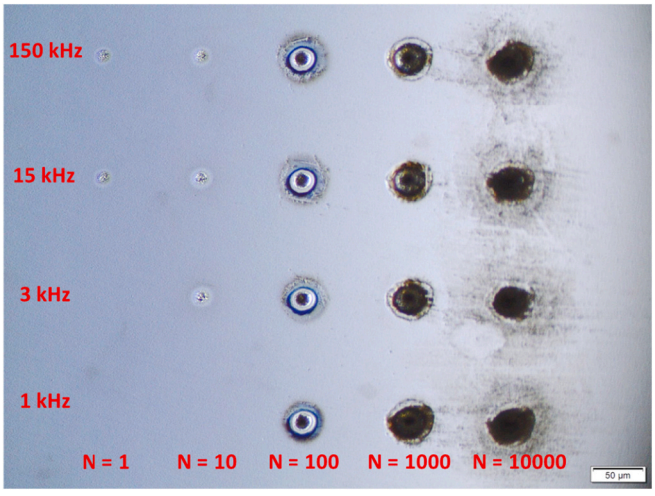

Fig. 1. Surface aspect of dimple-like micronotches machined by using different combinations of number of passes and frequency values.

3. Results and discussion

3.1. Dimensions, aspect ratio geometry and surface integrity of dimple-like and elongated micronotches

Specific goal was to reproduce dimple-like and elongated features of size similar to that estimated for the critical flaws, i.e. lower than 20 μm. Accordingly, laser processing parameters employed were frequency of 1 kHz and 100 passes. However, precision of the used equipment is limited, and well-defined geometry was only achieved for sizes higher than 40 μm. This was even more critical in the case of elongated micronotches. Here, well-defined tracks were achieved with geometry ratios (length/width) between 4 and 7. Although this artificially induced micronotches are slightly larger in size than effective critical defects, it is assumed that they are satisfactory for subsequent fracture mechanics and damage tolerance studies.

Detailed analysis of the shaped micronotches was conducted by FESEM (e.g. Fig. 2). A crown-like structure is observed in the case of dimple-like micronotches, whereas elongated micronotches show less overflow material above the surface of the sample. In both micronotch types, there appears to be remelted material inside them as well as a clear heat affected zone. The latter expands from the centre to the edges of the notches and leaves a grey-contrast area surrounding them.

3.2. Flexural strength and fractographic analysis of laser-micronotched specimens

Four specimens per notch type were tested to failure. One single micronotch was shaped in two of them, whereas three micronotches were machined in the other two samples. Single or multiple micronotches were introduced within the span of 10 mm where maximum tensile stresses are imposed at the surface during flexural testing in four-point bending. In the case of elongated micronotches, longer axis was aligned perpendicular to the longitudinal direction of the specimen. Flexural strength values of samples with shaped small-scale notches are given in Table 2. As expected, they were significantly lower than those determined on the pristine specimens, such relative difference being larger for samples containing the elongated micronotches.

FESEM inspection of broken surfaces allowed to identify the shaped micronotches as the critical failure sites (e.g. Fig. 3). Although elongated micronotches exhibited a rougher borderline than dimple-like ones, shape may be assumed to be effectively semi-elliptical, as originally attempted. Independent of micronotch geometry and size, two distinct regions are evidenced: one with a fused-like aspect and another one characterized by the observation of ductile dimples within the metallic binder of the hardmetal (Fig. 4). The former is a direct consequence of material removal and permanent microstructural modifications induced by shock waves [18,28], and similar to the scenario evidenced at the surface before mechanical testing. The latter is the result of nucleation, growth and coalescence of microcavities formed when stretching the metallic enclaves at the wake of propagating cracks, during unstable failure of cemented carbides [29–32].

Table 2
Flexural strength and relative critical flaw sizes (by comparison of experimentally measured and estimated values) for the specimens containing micronotches and tested to failure.

Micronotch type	Flexural strength (MPa)	Ratio between experimentally measured and estimated critical flaw size
Dimple-like	1226 ± 73	0.4–0.5
Elongated	588 ± 39	0.6–0.7

3.3. Fracture mechanics analysis of broken hardmetals containing laser-abladed small-scale flaws

It is well-established that rupture in hard and brittle-like materials is mainly associated with the existence of flaws and their ensuing propagation (e.g. Ref. [33]). These defects may be either intrinsic to processing or induced during service operation. Cemented carbides are manufactured through powder metallurgy routes; hence, processing-related flaws may be produced during powder preparation, mixing, consolidation, sintering, or subsequent surface finishing. A few particular examples of defects introduced during the processing of hardmetals are pores or cobalt-depleted carbide agglomerates (e.g. Ref. [25]). On the other hand, service-related defects are associated with surface or bulk integrity changes under operation, e.g. damage induced by oxidation, corrosion or thermal shock (e.g. Refs. [34–36]). Following the above ideas, fracture behavior of hardmetals may then be described by recourse to unstable propagation of existing flaws, independently of their origin and nature, within a LEFM framework. Such an approach is now implemented for further analysis and discussion of the experimental results just recounted.

To discern whether strength degradation measured simply results from the stress rising effect linked to the introduced micronotches, fracture results were analyzed by comparing estimated and observed critical flaw sizes (a_c), the latter as experimentally determined from FESEM examination. Calculations of a_c were based on the generic LEFM relationship [37]:

$$K_I = \sigma Y \sqrt{\frac{\pi a}{Q}} \tag{1}$$

$$Q \approx 1 + 1.464\left(\frac{a}{c}\right)^{1.65} \quad (a/c \leq 1) \tag{2}$$

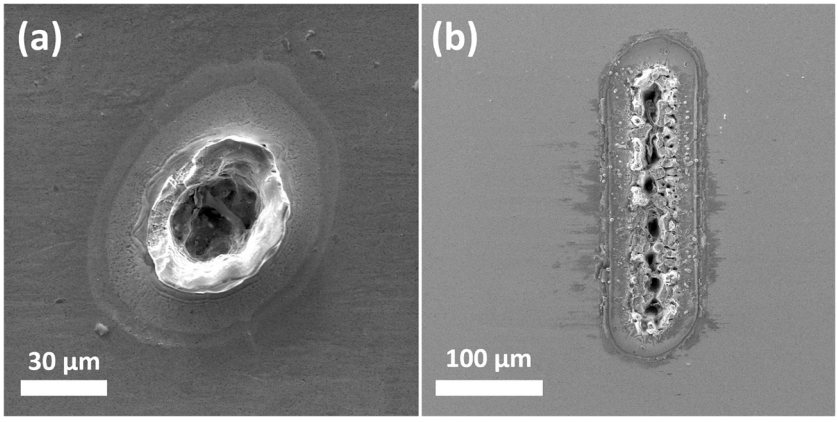

Fig. 2. SEM images of **(a)** dimple-like and **(b)** elongated micronotches.

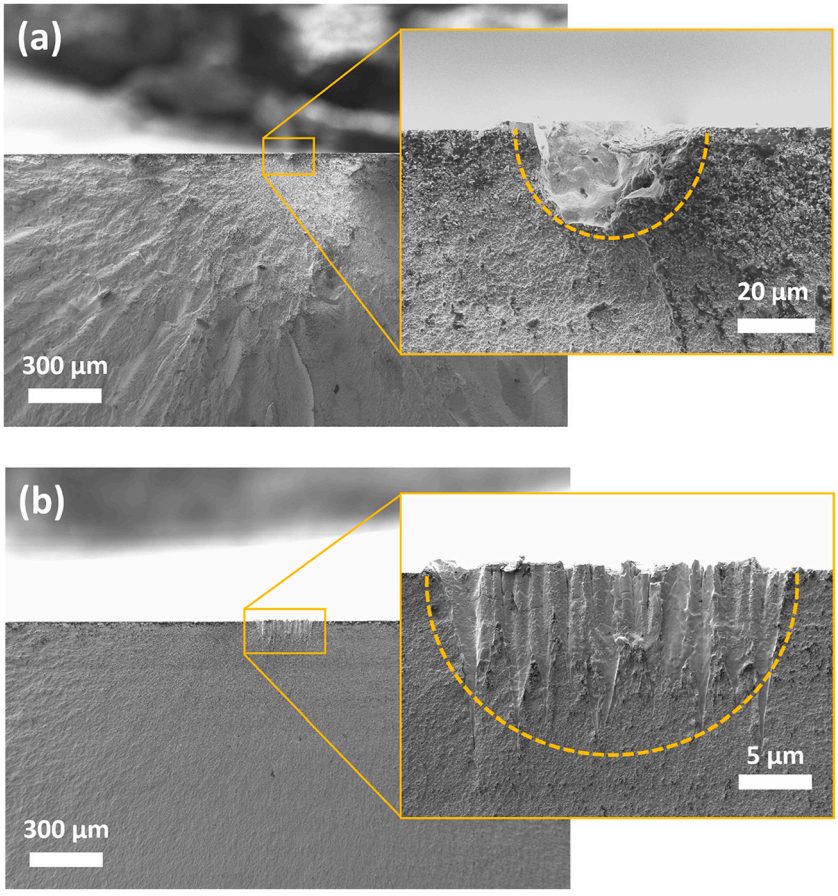

Fig. 3. FESEM micrographs of fracture surfaces for broken specimens containing **(a)** dimple-like and **(b)** elongated microntoches. Higher magnification images include schematic drawing of half-circular and half-elliptical flaws respectively, considered for determining dimensions of experimental critical defects, as well as for length/depth ratio to be used in the estimated values.

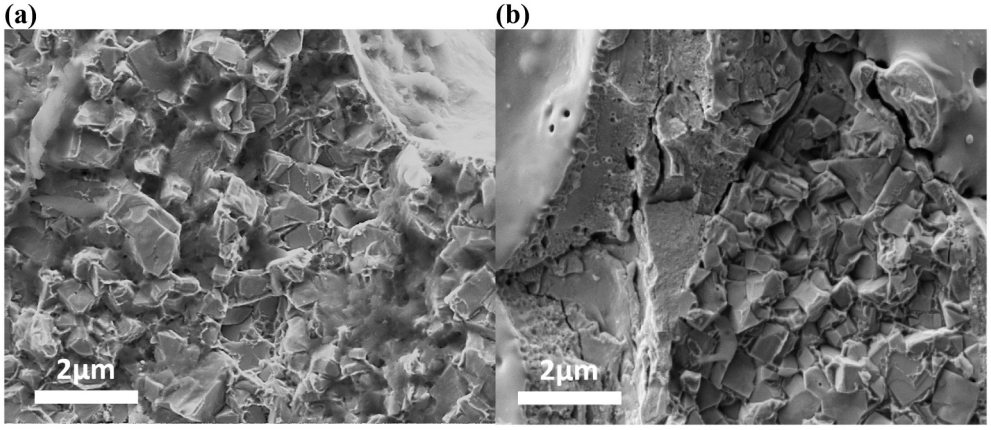

Fig. 4. High-magnification FEESEM micrographs showing specific fracture micromechanism features at the borderline between "fused/damaged" region and unstable failure for broken specimens containing **(a)** dimple-like and **(b)** elongated microntoches.

where K_I is the effective stress intensity factor, σ is the applied stress under four-point bending, a and c are the small and large radius of a half-elliptical crack, and Y has a value of 1.12.

Ratio values between observed and calculated critical flaw sizes for both micronotch types are included in Table 2. In both cases, experimentally determined critical flaw sizes are always smaller than the estimated ones. Beyond the scatter and uncertainties associated with experimental measurement and model simplifications, the above results suggest that besides the remote (outer surface) bending stress, laser-induced surface micronotches were also experiencing tensile residual stresses. The relative relevance of these residual stresses is clearly important for analyzing damage-induced (linked to laser ablation) strength degradation; thus, an estimation of their magnitude was attempted within a LEFM framework.

Laser-induced residual stresses may be roughly accounted from the experimentally measured failure-controlling data by using the principle of superposition of both applied far-field stress and residual stress intensity factors for the real critical flaw system, K_{app} and K_{res},

respectively, and equating the resulting total stress intensity factor (K_{tot}) to the fracture toughness of the material,

$$K_{tot} = K_{app} + K_{res} = K_{Ic} \quad (3)$$

Concerning K_{res}, residual stressess are assumed to be distributed uniformly over the contour of the laser-shaped micronotches. Additionally, because critical flaw sizes are much smaller than specimen height, boundary-correction factors for uniform tension (Y_{app}) and bending (Y_{res}) are taken to be equal. Under these considerations, Eq. (3) may now be written as:

$$K_{tot} = Y\left(\sigma_{app} + \sigma_{res}\right) = K_{Ic} \quad (4)$$

where σ_{res} represents an average residual stress magnitude.

Residual stress values for laser-micronotched specimens, as estimated via Eq. (4), yields values close to 500 and 150 MPa for dimple-like and elongated micronotches respectively, which are within the range of those reported in the literature for laser-treated cemented carbides. However, this simple analysis should rather be considered a preliminary proof of feasibility that laser technology may be implemented for surface machining of artificial small-scale flaws. Indeed, once heat-affected zone discerned in this study as well as solid phase transformation changes (in case heat input is too intensive) reported by Denkena and coworkers [12] are taken into account, it is clear that additional studies are required on the correlation among laser ablation effects on surface integrity, microstructural assemblage of hardmetals and operating parameters. They should allow to address and understand energy-related effects on microstructural changes and/or stress states of quite different magnitudes for cemented carbides. In this regard, it is very interesting to highlight the significant reduction of tensile residual stresses estimated for the specimens containing elongated micronotches, possibly as a consequence of self-annealing treatments linked to sequential micromachining of the surface notches.

4. Conclusions

Laser ablation technology has been proposed and successfully implemented for machining of artificial small-scale flaws in a fine-grained WC-11%wtCo hardmetal grade. Research conducted included preliminary optimization of laser machining parameters, particularly regarding number of passes and frequency. After combined and complementary optical and FESEM inspection of machined micronotches, optimized laser-ablation conditions have been selected on the basis of appropriated geometry and size, the latter within length scale of critical flaws identified in fractographic inspection of broken unnotched specimens. Once it has been achieved, they have been used for for introducing controlled damage-like features of cemented carbides. In this regard, flexural strength determined for micronotched samples have been analyzed through direct comparison of experimentally measured (from fractographic inspection) and estimated (within LEFM framework) sizes of critical flaws. It is found that small-scale micronotches shaped by laser ablation is a feasible option for fracture mechanics analysis of hardmetals, as far as residual stresses are taking into consideration. Within this context, and very interesting, laser-induced stresses are significantly reduced in the case of elongated micronotches, possibly as a consequence of self-annealing treatments linked to sequential micromachining of the surface notches.

Declaration of Competing Interest

The authors declare that they have no known competing financial interests or personal relationships that could have appeared to influence the work reported in this paper.

Data availability

The authors do not have permission to share data.

Acknowledgements

The research work was conducted within a cooperative effort between Xiamen Tungsten Co., Ltd. and Universitat Politècnica de Catalunya. L. Cabezas and S. Fooladi acknowledge Ph.D. scholarships received from the Spanish Ministerio de Ciencia e Innovación (Grant PRE2020-092445) and the Universitat Politècnica de Catalunya and Banco Santander (Predoctoral grant 2021 FPI-UPC_055), respectively.

References

[1] A.G. Evans, Perspective on the development of high-toughness ceramics, J. Am. Ceram. Soc. 73 (1990) 187–206, https://doi.org/10.1111/j.1151-2916.1990.tb06493.x.
[2] M.P. Rao, A.J. Sánchez-Herencia, G. Beltz, R.M. McMeeking, F.F. Lange, Laminated ceramics that exhibit a threshold strength, Science 286 (1999) 102–105, https://doi.org/10.1126/science.286.5437.102.
[3] A. Góez, D. Coureaux, A. Ingebrand, B. Reig, E. Tarrés, A. Mestra, A. Mateo, E. Jiménez-Piqué, L. Llanes, Contact damage and residual strength in hardmetals, Int. J. Refract. Met. Hard Mater. 30 (2012) 121–127, https://doi.org/10.1016/j.ijrmhm.2011.07.013.
[4] F. García-Marro, A. Mestra, V. Kanyanta, K. Maweja, S. Ozbayraktar, L. Llanes, Contact damage and residual strength in polycrystalline diamond (PCD), Diam. Relat. Mater. 65 (2016) 131–136, https://doi.org/10.1016/j.diamond.2016.03.004.
[5] A.-K. Hofer, R. Walton, O. Ševeček, G.L. Messing, R. Bermejo, Design of damage tolerant and crack-free layered ceramics with textured microstructure, J. Eur. Ceram. Soc. 40 (2020) 427–435, https://doi.org/10.1016/j.jeurceramsoc.2019.09.004.
[6] B.R. Lawn, S.K. Lee, I.M. Peterson, S. Wuttiphan, Model of strength degradation from Hertzian contact damage in tough ceramics, J. Am. Ceram. Soc. 81 (1998) 1509–1520, https://doi.org/10.1111/j.1151-2916.1998.tb02510.x.
[7] B.R. Lawn, Indentation of ceramics with spheres: a century after Hertz, J. Am. Ceram. Soc. 81 (1998) 1977–1994, https://doi.org/10.1111/j.1151-2916.1998.tb02580.x.
[8] A. Shyam, J.E. Allison, J.W. Jones, A small fatigue crack growth relationship and its application to cast aluminum, Acta Mater. 53 (2005) 1499–1509, https://doi.org/10.1016/j.actamat.2004.12.004.
[9] A. Kumar, M.C. Gupta, Laser machining of micro-notches for fatigue life, Opt. Lasers Eng. 48 (2010) 690–697, https://doi.org/10.1016/j.optlaseng.2010.01.008.
[10] B. Bode, W. Wessel, A. Brueckner-Foit, J. Mildner, M. Wollenhaupt, T. Baumert, Local deformation at micro-notches and crack initiation in an intermetallic g-TiAl-alloy, Fatigue Fract. Eng. Mater. Struct. 39 (2016) 227–237, https://doi.org/10.1111/ffe.12356.
[11] G. Dumitru, B. Lüscher, M. Krack, S. Bruneau, J. Hermann, Y. Gerbig, Laser processing of hardmetals: physical basics and applications, Int. J. Refract. Met. Hard Mater. 23 (2005) 278–286, https://doi.org/10.1016/j.ijrmhm.2005.04.020.
[12] B. Denkena, B. Breidenstein, L. Wagner, M. Wollmann, M. Mhaede, Influence of shot peening and laser ablation on residual stress state and phase composition of cemented carbide cutting inserts, Int. J. Refract. Met. Hard Mater. 36 (2013) 85–89, https://doi.org/10.1016/j.ijrmhm.2012.07.005.
[13] S. Fang, L. Llanes, D. Bähre, Laser surface texturing of a WC-CoNi cemented carbide grade: surface topography design for honing application, Tribol. Int. 122 (2018) 236–245, https://doi.org/10.1016/j.triboint.2018.02.018.
[14] B. Denkena, A. Krodel, L. Ellersiek, M. Murrenhoff, Production of chip breakers on cemented carbide tools using laser ablation, Proc. CIRP 94 (2020) 834–839, https://doi.org/10.1016/j.procir.2020.09.114.
[15] S. Fang, S. Klein, D. Bähre, L. Llanes, Performance of laser surface textured cemented carbide tools during abrasive machining: coating effects, surface integrity assessment and wear characterization, CIRP J. Manuf. Sci. Technol. 31 (2020) 130–139, https://doi.org/10.1016/j.cirpj.2020.10.006.
[16] M. Zimmermann, B. Kirsch, Y. Kang, T. Herrmann, J.C. Aurich, Influence of the laser parameters on the cutting edge preparation and the performance of cemented carbide indexable inserts, J. Manuf. Process. 58 (2020) 845–856, https://doi.org/10.1016/j.jmapro.2020.09.003.
[17] K.E. Hazzan, M. Pacella, T.L. See, Laser processing of hard and ultra-hard materials for micro-machining and surface engineering applications, Micromachines 12 (2021) 895, https://doi.org/10.3390/mi12080895.
[18] L. Ortiz-Membrado, C. Liu, J. Prada-Rodrigo, E. Jiménez-Piqué, L.L. Lin, P. Moreno, M.S. Wang, L. Llanes, Assessment of fracture toughness of cemented carbides by using a shallow notch produced by ultrashort pulsed laser ablation, and a comparative study with tests employing precracked specimens, Int. J. Refract. Met. Hard Mater. 108 (2022), 105949, https://doi.org/10.1016/j.ijrmhm.2022.105949.
[19] B.N. Chichkov, C. Momma, S. Nolte, F. von Alvensleben, A. Tünnermann, Femtosecond, picosecond and nanosecond laser ablation of solids, Appl. Phys. A Mater. Sci. Process. 63 (1996) 109–115, https://doi.org/10.1007/s003390050359.
[20] J. Meijer, K. Du, A. Gillner, D. Hoffmann, V.S. Kovalenko, T. Masuzawa, A. Ostendorf, R. Poprawe, W. Schulz, Laser machining by short and ultrashort

pulses, state of the art and new opportunities in the age of the photons, CIRP Ann. 51 (2002) 531–550, https://doi.org/10.1016/S0007-8506(07)61699-0.
[21] D. Bäuerle, Laser Processing and Chemistry, Springer Berlin, Heidelberg, 2011, https://doi.org/10.1007/978-3-662-04074-4.
[22] Z.Z. Fang, Correlation of transverse rupture strength of WC–Co with hardness, Int. J. Refract. Met. Hard Mater. 23 (2005) 119–127, https://doi.org/10.1016/j.ijrmhm.2004.11.005.
[23] M. Jonke, T. Klünsner, P. Supancic, W. Harrer, J. Glätzle, R. Barbist, R. Ebner, Strength of WC-Co hard metals as a function of the effectively loaded volume, Int. J. Refract. Met. Hard Mater. 64 (2017) 219–224, https://doi.org/10.1016/j.ijrmhm.2016.11.003.
[24] W. Tang, L. Zhang, Y. Chen, H. Zhang, L. Zhou, Corrosion and strength degradation behaviors of binderless WC material and WC–Co hardmetal in alkaline solution: a comparative investigation, Int. J. Refract. Met. Hard Mater. 68 (2017) 1–8, https://doi.org/10.1016/j.ijrmhm.2017.06.003.
[25] J.M. Tarragó, D. Coureaux, Y. Torres, E. Jiménez-Piqué, L. Schneider, J. Fair, L. Llanes, Strength and reliability of WC-Co cemented carbides: understanding microstructural effects on the basis of R-curve behavior and fractography, Int. J. Refract. Met. Hard Mater. 71 (2018) 221–226, https://doi.org/10.1016/j.ijrmhm.2017.11.031.
[26] Y. Torres, D. Casellas, M. Anglada, L. Llanes, Fracture toughness evaluation of hardmetals: influence of testing procedure, Int. J. Refract. Met. Hard Mater. 19 (2001) 27–34, https://doi.org/10.1016/S0263-4368(00)00044-5.
[27] Y. Torres, J.M. Tarrago, D. Coureaux, E. Tarrés, B. Roebuck, P. Chan, M. James, B. Liang, M. Tillman, R.K. Viswanadham, K.P. Mingard, A. Mestra, L. Llanes, Fracture and fatigue of rock bit cemented carbides: mechanics and mechanisms of crack growth resistance under monotonic and cyclic loading, Int. J. Refract. Met. Hard Mater. 45 (2014) 179–188, https://doi.org/10.1016/j.ijrmhm.2014.04.010.
[28] M. Turon-Vinas, J. Morillas, P. Moreno, M. Anglada, Evaluation of damage in front of starting notches induced by ultra-short pulsed laser ablation for the determination of fracture toughness in zirconia, J. Eur. Ceram. Soc. 37 (2017) 5127–5131, https://doi.org/10.1016/j.jeurceramsoc.2017.07.006.
[29] L.S. Sigl, H.E. Exner, Experimental study of the mechanics of fracture in WC–Co alloys, Metall. Trans. A. 18A (1987) 1299–1308, https://doi.org/10.1007/BF02647199.
[30] L.S. Sigl, H.F. Fischmeister, On the fracture toughness of cemented carbides, Acta Metall. 36 (1988) 887–897, https://doi.org/10.1016/0001-6160(88)90143-5.
[31] J.M. Tarragó, E. Jiménez-Piqué, L. Schneider, D. Casellas, Y. Torres, L. Llanes, FIB/FESEM experimental and analytical assessment of R-curve behavior of WC–Co cemented carbides, Mater. Sci. Eng. A645 (2015) 142–149, https://doi.org/10.1016/j.msea.2015.07.090.
[32] J.M. Tarragó, D. Coureaux, Y. Torres, D. Casellas, I. Al-Dawery, L. Schneider, L. Llanes, Microstructural effects on the R-curve behavior of WC-Co cemented carbides, Mater. Design 97 (2016) 492–501, https://doi.org/10.1016/j.matdes.2016.02.115.
[33] B. Lawn, Fracture of Brittle Solids, 2nd ed., Cambridge University Press, Cambridge, U.K., 1993.
[34] B. Casas, X. Ramis, M. Anglada, J.M. Salla, L. Llanes, Oxidation-induced strength degradation of WC–Co hardmetals, Int. J. Refract. Met. Hard Mater. 19 (2001) 303–309, https://doi.org/10.1016/S0263-4368(01)00033-6.
[35] J.M. Tarragó, G. Fargas, L. Isern, S. Dorvlo, E. Tarres, C.M. Müller, E. Jiménez-Piqué, L. Llanes, Microstructural influence on tolerance to corrosion-induced damage in hardmetals, Mater. Design 111 (2016) 36–43, https://doi.org/10.1016/j.matdes.2016.08.066.
[36] J.M. Tarragó, S. Dorvlo, J. Esteve, L. Llanes, Influence of the microstructure on the thermal shock behavior of cemented carbides, Ceram. Int. 42 (2016) 12701–12708, https://doi.org/10.1016/j.ceramint.2016.05.024.
[37] J. Newman, I. Raju, An empirical stress-intensity factor equation for the surface crack, Eng. Fract. Mech. 15 (1981) 185–192.